Sic. J. Fac. Sci., Menufiya Univ. Vol. XVI (2002) (43 – 78)

Thermal Properties of Binary Tellurite Glasses

R.El-Mallawany, A.Abdel-Kader, M.El-Hawary and N. El-Khoshkhany.

Physics Dept., Faculty of Science, Menoufia Univ., EGYPT.

Abstract:

Binary tellurite glass systems of the forms $TeO_2(100-x)-xA_nO_m$ where A_nO_m = La_2O_3 or V_2O_5 and x = 5,7.5,10,12.5,15,17.5 and 20 mol.% for La_2O_3 and 10,20,25,30,35,40,45 and 50 mol.% for V_2O_5 were prepared. Density and molar volume of each glass were measured and calculated. DSC at different heating rates was used to gain some insight into the thermal stability and calorimetric behavior of the present binary transition metal and rare earth tellurite glasses. The glass transformation temperature T_g and glass crystallization temperature T_c were recorded at different heating rates, the glass transition activation energy and the glass crystallization activation energy were calculated by different methods.

1- Introduction:

Tellurite glasses exhibit a range of unique properties of potential applications as pressure sensors or as new laser hosts. Although the physical properties and structure of crystalline solids are now understood in essence, this is not the case for amorphous materials. The considerable theoretical difficulties experienced for amorphous solids are amplified by the lack of precise experimental information. To fill this gap, the present work is carried out. The mutual benefits of the proposed cooperative research effort are seen as providing the fundamental base for finding new optical glasses with new applications especially (Tellurite-Based Glass Optical Fiber) which are of interest of all countries all over the world. The recent boo "Telurite Glass Handbook; Physical Properties and data", (2001)

[1] collected the physical properties of some tellurite glasses.

2- Experimental Work:

2.1. Glass Preparation, Vitreous State Density Measurements:

The binary glass system $(100-x)TeO_2-(x)A_nO_m$ was prepared by mixing all specified weights of tellurium oxide (TeO_2, 99.99% purity, BDH), A_nO_m =Lanthanum oxide (La_2O_3, 99,99 purity, BDH) where x = 5 ,7.5 ,10 ,12.5 ,15 ,17.5

and 20 mol% and vanadium oxide (V_2O_5, 99,99 purity, BDH) where x = 10, 20, 25, 30, 35, 40, 45 and 50 mol% . The diffusion process took place through an agate mortar and the mixture was thoroughly ground for 20 minutes. The powdered mixture was then put in an alumina crucible and heated in a melting furnace. In order to reduce any tendency of volatilization, the mixture was kept at 300 ^{0}C for 15 minutes. The crucible was then kept in the same furnace above 300 ^{0}C, the value of these temperature depend upon the composition of each sample and its melting temperature. After reaching the required temperature (850-900 ^{0}C), the mixture was left for 20 minutes. To improve the homogenity, the melt was stirred from time to time with an alumina rod. The melt which had a high viscosity was cast at room temperature in a split mould made from mild steel. The sample was transferred after that to the annealing furnace. After 1h. at 300 ^{0}C, the annealing furnace was then switched off and the glass rod was allowed to cool inside it for 24 h. The two glass opposite faces were ground roughly approximated parallel on a lapping machine with 600grade SiC powder. Opposite faces were finished optically flat and parallel with a high mirror- like surface. As both the preparation and annealing furnace had capacities greatly exceeding the volume of the crucible, the temperature gradients in the volume of the crucible, the temperature gradients across the glass at any time during melting and annealing were constant. The glass formed was therefore expected to be homogeneous. Table (1) gives the composition of the glass sample investigated in the present work.

The vitreous state of two binary systems was examined by X-ray using a Shimadzu diffractometer (Model XD-3). The density of the prepared glassy samples was determined at room temperature by a simple Archimedes method, using toluene as an immersion liquid. The density of each composition was then obtained by using the relation,

$$\rho_g = \frac{W_a \rho_L}{(W_a - W_L)} \qquad (1)$$

Where ρ_L is the relative density of the liquid toluene (0.864 gm/cm^{-3} at 25^{0}C), W_a

and W_L are the weights of the glass sample in air and in the liquid respectively. The molar volume *V* (i.e., the volume occupied by one gram molecule of the glass), was calculated by the following expression:

$$V = \frac{(xM_A + yM_B)}{\rho_g} \qquad (2)$$

Where, the glass composition is represented by x and y and x+y =100% and M_A, M_B are the molecular weights of materials *A* and *B* forming the glassy network.

2.2. Thermal Measurement:

The thermal behavior was investigated using differential scanning calorimetric (Shimadzu 50 DSC). The temperature and energy calibrations of the instrument were performed using the well known melting temperature and melting enthalpy of high purity indium metal. The calorimetric sensitivity is 10 μw and the temperature accuracy is ±1.0 K. The crystallization thermogram of the sample was recorded as the temperatures of the samples were increased at a uniform heating rate α at 5, 10, 15 and 20 K/min. Typically than 50 μw was scanned over a temperature range from room temperature to about 500K. The melting temperature was determined by using differential thermal analysis (Shimadzu 30 DTA).

3-Results and Discussion:

The X-ray diffraction tests of the prepared glasses in the powder form don't show any peaks, indicating that the structures of the prepared samples are, in generally, amorphous.

3.1. Density and Molar volume Results:-

The results of the density measurements for the produced glasses are shown in Fig.(1-a&b). Table (1) shown the variation of both density and molar volume for all glasses collected for both binary tellurite glass series, and for pure TeO_2 glass [2]. It is informative to compare the densities of pure TeO_2 crystal and the pure TeO_2 glass [3]; the ratio of this parameter was calculated 1.18 [2]. The fact that the density of the glass was smaller than that of the crystal correlates extremely well with the reduced number of TeO_2 units that could be accommodated

in the more open structure of the vitreous state. For binary (La_2O_3 and V_2O_5), tellurite glasses both ρ and *V* depended on the percentage and type of modifier used. The results showed that the density increased from 5.18 to 5.64 g/cm^3 with increasing La_2O_3 content (5 to 20) mol%. The density also decreased from 5.04 to 4.01 g/cm^3 with the increase of V_2O_5 (10 to 50) mol%.

This change in density accompanying the addition of La_2O_3 or V_2O_5 is due to the change in the atomic mass and atomic volume of constituent elements. The atomic mass of Te, La and V atoms are 127.6, 138.91 and 50.942 respectively and their atomic radii are 1.6, 1.87 and 1.34Å respectively. This explains the observed increasing and decreasing with increasing La_2O_3 or V_2O_5 content. The molar volume *V* was calculated from Eq.(2). The change of molar volume versus mol% concentration of La_2O_3 and V_2O_5, are shown in Fig.(2-a&b) respectively. The calculated molar volume of the pure TeO_2 crystal and TeO_2 glass were 26.6 and 31.29 cm^3 [4], respectively. This means that the ratio $V_{(glass)}/V_{(crystal)}$ is 1.18 [5], i.e., the change is only 18% from crystalline solid to be non-crystalline solid. Hence, the fact that molar volume of the glass is greater than that of the crystal which correlates extremely well with longer number of TeO_2-units that can be accommodated in the more open structure of the vitreous state. For the first series of binary TeO_2-La_2O_3 ; the molar volume increased from 32.42 cm^3 to 34.21 cm^3. Also for the second series TeO_2-V_2O_5 glass, the molar volume increased from 32.11 cm^3 to 42.58 cm^3 as shown in Fig.(2-a&b). The molar volume of binary TM (transition metal) or RE (rare earth) tellurite glasses would be higher than pure TeO_2 glass, as shown in Table (1).

The structural interpretation will be based on the simple model of compressibility by Mukherjee [6] of binary glass A_xB_{1-y} containing n_A formula units of type *A* and n_B formula units of type *B* with the percentage $x=n_A/(n_B+n_A)$ has stated a relation to find the volume. The volume of the binary glass containing n_A (Avogadro's number) formula units of type *A* and n_B formula unit of type *B* can be easily determined from the density measurements using the relation,

$$V = \frac{[M_A + (n_B / n_A)M_B]}{\rho} \qquad (3)$$

Where ρ is the density of the binary glass A_XB_{1-X}, and M_A and M_B, are the molecular weights of the formula units *A* and *B* respectively, and (*x*) is the percentage. The model supposed that the composition of binary glass *AB* changes from n_A and n_B formula units of types *A* and *B*, respectively, to (n_A-1) and $(n_B + 1)$ corresponding formula units. While the total number of formula units of *A* and *B* taken together remains unchanged, the volume of the vitreous system changes by an amount which called the difference volume V_d due to the exchange of one formula unit between *A* and *B* in the binary glass system. The compressibility model assumed that the difference volume V_d and the mean volume V_A per formula unit of *A* in the binary glass A_XB_{1-X} independent of the percentage of the modifier for a glass series and different from series to another. Also, the model restricted that the binary glass series has the same structure and no phase changes. This implies that the volume *V* of the binary system A_XB_{1-X} containing n_A (Avogadro's number) formula units of *A* and n_B formula units of B has been written as:

$$V = n_A V_A + n_B (V_d + V_A)$$

$$= V_0 + (n_B / n_A)(n_A V_d + V_0) \qquad (4)$$

where, $V_0 = n_A V_A$ represents the molar volume of the vitreous system consisting of n_A formula units of type *A* only with the mean volume equal to V_A per formula unit and (n_B/n_A) is the composition ratio. Although we do envisage the molecular units in the glass network, where *A* stands for the glass former TeO_2 and *B* stands for the modifier, i.e., any one of La_2O_3 or V_2O_5. Eq.(4) clearly indicates that the plot of *V* against the composition ratio (n_B/n_A) follows a straight line from which the intersect with Y-axis gives V_0 and the slope gives $(n_A V_d + V_0)$. From table (1), Fig.(3-a&b) it was found that, for the two binary tellurite glasses studied in the present investigation, the value of V_0 is 32.1717cm^3 from the line of TeO_2-La_2O_3 and 31.3645cm^3 for the line TeO_2-V_2O_5, respectively. The calculated values of the volume obtained from the sample model agreed with the experimental values of the pure TeO_2 [4]. From the slope of both lines in Fig.(3-a&b) and by

using Eq.(4), the values of the quantity ($n_A V_d$) are (-24.373 cm^3) and (-19.396 cm^3) for the two binary glass series, respectively. These values are negative while binary V_2O_5-P_2O_3 glasses have the value of (+9.538 cm^3) as stated by [6]. This change in molar volume was due to the change in the structure caused by the change on interatomic spacing, which could be attributed to the change in the number of bonds per unit volume of the glassy network and change of the stretching force constant of the bonds inside the glassy network. El-Mallawany [5] has used Mukherjee model and has calculated V_0 of pure TeO_2 and also for the binary TeO_2 –MoO_3 glasses. The calculated value of V_A for pure TeO_2 is equal 10.41 cm^3 and for (20 mol % TeO_2–MoO_3, V_A = 9.76 cm^3, 50 mol% V_A = 9.4 cm^3) while for (20 mol% TeO_2-V_2O_5, V_A = 9.3 cm^3, 50 mol% V_A = 8.54 cm^3).

Now for more quantitative analysis, we calculate N_b; is the number of bonds per unit volume of the glass given by

$$N_b = \sum n_f (N_f) = \sum n_f \left\{ \frac{N_A \rho}{M_g} \right\} \quad (5)$$

Where, n_f is the number of network bonds per unit glass formula and equal to the coordination number of each cation times the number of cations in the glass formula unit. N_f is the number of formula units per volume, N_A is Avogadro's number, ρ is the glass density and M_g is the molecular weight of the glass. Fig.(4-a&b) show a plot of number of bonds per unit volume versus mol.% concentration of La_2O_3 and V_2O_5, respectively. After calculating these parameter, we conclude that the number of network bonds per unit volume, N_b, equals $7.74.10^{22}$ cm^{-3} for pure TeO_2 glass. For binary glass TeO_2 -La_2O_3 the number of network bonds per unit volume increased from ($8.07x10^{22}$ to $9.58x10^{22}$ cm^{-3}) with increasing La_2O_3 content from (5 to 20 mol%), and for TeO_2-V_2O_5 the number of network bonds per unit volume decreased from ($7.69x10^{22}$ to $6.36x10^{22}$ cm^{-3}) with increasing V_2O_5 content from (10 to 50 mol%). The average force constant of the glass was given by the relation:

$$\overline{F} = \frac{f_1 (n_1)(N_c)_1 + f_2 (n_2)(N_c)_2}{(n_1)(N_c)_1 + (n_2)(N_c)_2} \quad (6)$$

where f, is the stretching force constant (calculated according to the empirical relation $f=17/r^3$ from Ref. [7]), where, r is the ionic bond length), $(N_C)_1$ is the number of cations per glass formula unit, $\Sigma_i (N_C)_i = x\, n_1 + (1-x)n_2$, for the multicomponent tellurite glasses in the form $xA_{n1}O_{m1} - (1-x)G_{n2}O_{m2}$, (where x is the mole fraction). Fig.(5-a &b) and show a plot of average force constant versus mol.% concentration of La_2O_3 and V_2O_5 respectively. The average forces constant of TeO_2-La_2O_3 was decreased from (196.7 to 160.5 N/cm) with increasing La_2O_3 content from (5 to 20 mol%), and was increased from (234.8 to 264.8 N/cm) with increasing V_2O_5 content from (10 to 50 mol%). The quantitative analysis can be summarized as follows: for R.E-tellurite glasses, the structure of the glass Is weaker and more linked; the density data and molar volumes show that rare earth oxides act as a network former rather than a network modifier in tellurite glass by increasing the crosslink density of TeO_2. For T.M.-tellurite glasses the density was decreased while the molar volume would be higher than pure TeO_2 glass, as shown in Table (1). From the change in the molar volume it was clear that the corresponding structural units with its surrounding space, increased by introducing TM oxides into the tellurite network, i.e. the basic structural units are linked more randomly.

3.2.Thermal:-

The DSC curves for the glasses are shown in Fig.(6-a&b), for TeO_2-La_2O_3, and in Fig.(7-a&b) for TeO_2-V_2O_5. The curves show a very broad endothermic peak corresponding to the glass transition which is characterized by the temperature, T_g. As shown in Fig.(7-a), this transition is followed by more than one exothermic peak corresponding to several crystallization temperatures, T_c. The two main successive crystallization peaks observed by increasing of V_2O_5 mol%. This shows different stages of crystallization, in coincidence with previous work [8], and that some tellurite glasses are characterized by more than one crystallization mechanism. The first exothermic peak may be attributed to nucleation processes followed by the formation of a crystalline phase having a low internal free energy. The second peak at a higher temperature is attributed to the formation of a more

relaxed crystalline phase. The approximate crystallization kinetics can be considered as follows. TeO_2 crystallizes in two main modifications [9]: orthorhombic β-TeO_2 (tellurite) and tetragonal α-TeO_2 (paratellurite) [10] In both forms, the basic coordination polyhedron is a slightly distorted traigonal bipyramid with one equatorial position occupied by a one electron pair. The dependence of T_g on the type of modifier is given in Table (2). The increases in T_g induced by addition of the modifier could be explained by the increased degree of polymerization. T_c, the temperature at which the crystallization process started was determined for the present glasses, see Table (2).

The values of the difference between T_g and T_c were calculated to illustrate the size of the working range between T_g and T_c. For pure TeO_2 glass $T_c - T_g$ =75 $^{\circ}K$ [2] and in the present work changed from (89 $^{\circ}K$ to 22 $^{\circ}K$) and from (74 $^{\circ}K$ to 167 $^{\circ}K$) for binary tellurite -La_2O_3 and -V_2O_5, respectively. The values of T_m for all glasses obtained from the DTA curves were in the range of (917 $^{\circ}K$ to 1180 $^{\circ}K$), as shown in Table (2). The values of T_g/T_m were in the range of (0.43 to 0.68). The glass-forming tendency, K_g, which was a useful parameter in comparing the devitrification tendency of the glass, is given by:

$$K_g = \frac{T_c - T_g}{T_m - T_c} \qquad (7)$$

and had the values of (0.54- 0.2). As can be seen from Table (3), low values of K_g suggested high tendencies to devitrifies. Previously, El-Mallawany [2] has calculated K_g for other binary tellurite TM tellurite glasses of the form TeO_2- MoO_3, TeO_2-Co_3O_4 and TeO_2-MnO_2. The value of K_g were (0.46 to 0.41), (0.33 to 0.31) and from (0.45 to 0.4) respectively. The glass-forming tendency K_g of the present binary tellurite glasses decreases from (0.54 to 0.29) for RE tellurite glasses system. The behavior is absolutely opposite in the second binary glass series become K_g increases from (0.3 to 0.43). Also the glass transition temperature, the activation energy of the glass transition E_t and the crystallization activation energy

E_c will be evaluated according different models as stated in next sub section.

Also, it is very important to analyze the variation of T_g in both tellurite glasses series as a function of both N_b and $\overline{F}$, i.e.,

$$T_g = f(N_b, \overline{F}) \qquad (8)$$

From Tables (1&2) it is clear that, for binary glass TeO_2 -La_2O_3 the glass transition temperature, T_g increased from (623K to 698K), the number of network bonds per unit volume N_b, increased from (8.069×10^{22} cm^{-3} to 9.584×10^{22} cm^{-3}) and the average forces constant $\overline{F}$, decreased from (196.7 N/cm to 160.5 N/cm) with increasing La_2O_3 content from (5 to20 mol%). While for TeO_2-V_2O_5 the glass transition temperature T_g decreased from (565K to 510 K), the number of network bonds per unit volume N_b, decreased from (8.35×10^{22} cm^{-3} to 6.36×10^{22} cm^{-3}) and the average forces constant $\overline{F}$, increased from (234.8 N/cm to 264.8 N/cm) with increasing V_2O_5 content from (10 to 50 mol%).

3.2.1.Glass Transition Temperature and Glass Transition Activation Energy:-

The dependence of T_g on the heating rate α can be followed according to the empirical formula [11], as shown in Eq. (9).

$$T_g = A + B\ln(\alpha) \qquad (9)$$

Where *A* and *B* are constant for a given glass composition. The dependence of T_g on α is shown in Fig.(8-a&b) which indicates a relationship for the prepared glasses. Although the dependence of T_g on the heating rate α of the binary glasses were found to follow the Eq.(10) which stated by. Chen [12] and has often been used to calculate glass transition activation energy (E_t). Plots of $\ln(\alpha/T_g^2)$ versus $1/T_g$ for prepared tellurite glasses indicate linearity as shown in Fig.(9-a&b), the obtained values of E_t are showed in Table (3), E_t has been also calculated using the expression by Moynihan [13] as in Eq.(11)

$$\ln\left(\alpha / T_g^2\right) = \left(-E_t / RT_g\right) + const.$$

$$\ln(\alpha) = (-E_t / RT_g) + const. \quad (11)$$

Fig.(10-a&b) show the relation between ln(α) and $1/T_g$ for the prepared glasses. The values of E_t deduced from this relation are obtained in Table (3). It is clear from the obtained data for the glass transition transformed temperature T_g at heating rate 5 K/min that the T_g depends upon:

- Tellurite glasses with higher percentage of La_2O_3 has the higher values of T_g, and with higher percentage of V_2O_5 has the lower values of T_g, i.e. La_2O_3 create a more strengthen tellurite glass.
- The glass transition activation energy E_t of La_2O_3 tellurite glass has been increased from 286.5 kJ/mol to 423.7 kJ/mol by increasing La_2O_3 from 5 to 20 mol.% [by using Moynihan model] while it has been increased from 276.38 kJ/mol to 411.67 kJ/mol for the same amount of La_2O_3 [by using Chen model], so both models confirm each other.

Also the glass transition activation energy E_t of V_2O_5 tellurite glasses has been decreased from 594.96 kJ/mol to 289.79 kJ/mol by increasing V_2O_5 from 10 to 50 mol% [by using Moynihan model], while it has been decreased from 585.58 kJ/mol to 281.25 kJ/mol for the same amount of V_2O_5 [by using Chen model], so both models confirm each other.

3.2.2. Crystallization Temperature and Crystallization Activation Energy:-

The method which is commonly, used in analyzing crystallization data in DSC and DTA experiments developed by Kissinger [20,21]. While the method proposed by Ozawa [22] is used to deduce the order of the crystallization reaction (n) at constant temperature,

$$d\{\ln[-\ln(1-\chi)]\} / d\{\ln(\alpha)\} = -n \quad (12)$$

Where α is heating rate of binary glass and χ is the volume fraction crystallized in time t.

On this basis, plotting $\ln[-\ln(1-\chi)]$ versus ln(α), which is obtained at the same temperature from a number of crystallization exotherms taken at different heating rates should yield the value of n .

Now to deduce the order of crystallization, the value of (n) is evaluated by plotting ln[-ln(1-χ)] versus ln(α), where χ is obtained from the crystallization exothermic peaks at the same temperature taken at deferent heating rates. Fig.(11-a&b) show the plots of ln[-ln(1-χ)] versus ln(α) at different constant values of temperature. From the slopes of this relation, the value of (n) is equal 0.93, 1.38, 1.15, 1.18, 1.05 and 1.14 respectively by increasing La_2O_3 from 5 to 17.5 mol.%, while (n) is equal 2.17, 2.11, 2.12, 2.01, 1.91, 1.90 and 2.17 respectively at the first crystallization peaks by increasing V_2O_5 from 10 to 50 mol.% and at the second crystallization peaks (n) is equal 2.33 and 3.31 for 45 and 50 mol.% of V_2O_5.

The values of the crystallization activation energy (E_c) calculated by using methods of Coast- Redfern- Sestak [23,25], Kissinger [20,21] and modified Ozawa-Chen [19,12]. The values of Crystallization Activation Energy E_c calculated for all the heating rates by using method of Coast- Redfern- Sestak [21-23]. Fig.(12-a&b) show the plots of ln[-ln(1-χ)] versus $1/T$, at different heating rates, from the slopes the average values of the crystallization activation energy of the prepared glasses for the 1^{st} crystallization peak are calculated and obtained in Table (4). The values of the crystallization activation energy (E_c) calculated using Kissinger method and modified Ozawa-Chen equation from Fig.(13-a&b) and Fig.(14-a&b) are obtained in Table (4). It has been found that the crystallization activation energy E_c ,using Kissinger method, increased from 342.138 kJ/mol to 531.745 kJ/mol due to increasing of La_2O_3 in the glasses from 5 to 17.5 mol.%. Also the same behavior by Ozawa-Chen model ,and Coast- Redfern- Sestak are found. But due to increasing of V_2O_5 in the glasses from 10 to 50 mol.% the first crystallization activation energy E_{c1} decreased from 458.933 kJ/mol to 174.594 kJ/mol. The second crystallization activation energy E_{c2} is equal 318 kJ/mol and 332 kJ/mol at 45 and 50 V_2O_5 mol.%. Also the same behavior by Ozawa-Chen model and Coast- Redfern- Sestak are found. In accordance with the strained mixed heating rates for prepared glasses $(TeO_2)_{100-x}$-$(V_2O_5)_x$. Cluster model of Goodman [26], the vitreous state of these glasses may in some way consist of a

mixture of extremely small crystallites of size less than 10 nm of the two polymorphic phases of TeO_2, which forms the essential framework of the glass matrix, together with small regions proportional to the concentration of the added modifier. As the temperature is raised to the point at which significant solid state diffusion of atoms or groups of atoms can occur, that is above T_g, the diffusion of clusters of size < 3 nm, together with statistical collisions between them, result in these clusters coalescing. Clusters which differ very little in free energy and orientation collide in such a way that interfaces with minimum strain are established between them. Such an assemblage of clusters results in partial crystallization, as the α-TeO_2 phase is formed. Above the first crystallization peak, there is still some persisting amorphous phase, representing the remaining clusters of the other polymorphic phase of TeO_2 with more highly strained interfaces. On a further increase in temperature, these highly strained interfaces have the opportunity to relax. Such relaxation occurs by acquiring atoms with the appropriate orientation and releasing the strain in the interfaces the neighboring clusters and to the liquid phase. In this way, through statistical collisions clusters of the remaining polymorphic phase could assemble with minimum or zero strained interfaces and crystallize to form β-TeO_2. This second stage of crystallization is observed as the second weak exothermic peak, in the glasses containing Vanadium oxide.

Conclusion:

The glass transformation temperature and crystallization temperature have been measured for the binary transition metal and rare earth tellurite glasses. The glass transformation energy has been calculated using Chen's and Moynihan's formulas. Both models are very close for every glass series. Also, the crystallization energies of these glasses have been calculated using Kissinger's, Ozawa-Chen's and Coast-Redfern-Sestak's models.

References :

1. R. El-Mallawany, "Tellurite Glass handbook: Phyical Properties and Data", publish by CRC Press, FL, USA, (2001).
2. R. El-Mallawany, J. Mat. Sci. in Electronics, 6, 1, (1995).

3. E. Havinga, J. Phys. Chem. Solids, 18, 253, (1961).
4. E. F. Lambson, G. A. Saunders, B. Bridge and R.A. El-Mallawany, J. Non-Cryst. Solids, 69, 117, (1984).
5. R. El-Mallawany, Phys. Stat. Sol.(a), 177, 439, (2000).
6. S. Mukherjee, U. Ghosh and C. Basu, J. Mater. Sci. Lett., 11, 985, (1992).
7. B. Bridge and A. A. Higazy, J. Phys. Chem. Glasses, 27, 1, (1986).
8. V. S. Kozhukharov, S. Nikolov and M. Marinov, J. Mater. Res. Bull. 14, 735, (1979).
9. H. Beyer, Z. Kristallogr. 124, 228, (1967).
10. P. A. V. Johnson, A. C. Wright, C. A. Yarker and R. N. Sincair, J. Non-Cryst. Solids 81, 163, (1986).
11. Giridhar, S. Mahadevan and A. K. Singh, J. Non-Cryst. Solids, 88, 11, (1986).
12. H. Chen, J. Non-Cryst. Solids, 27, 257, (1978).
13. C. T. Moynihan, A. J. Easteal, J. Wider and J. Tucker, J. Phys. Chem. 78, 2673, (1974).
14. W. A. Johson and K. F. Mehl, Trans. Am. Inst. Mining Met. Engns., 135, 315, (1981).
15. M. Avrami, J. Chem. Phys., 7, 1103, (1939).
16. M. Avrami, J. Chem. Phys., 9, 177, (1941).
17. S. Mahadevan, A. Giridhar and A. K. Singh, J. Non-Cryst. Solids, 88, 11, (1986).
18. H. Yinan and D. R. Uhlmann, J. Non-Cryst. Solids, 54, 253,(1983).
19. T. Ozawa, Bull. Chem. Soc. Jpn. 38, 1881, (1965).
20. H. E. Kissinger, J. Res. NBS, 57, 217, (1956).
21. H. E. Kissinger, Anal. Chem., 29, 1702, (1957).
22. T. Ozawa, Polymar,12, 150, (1971).
23. W. Coats and J. P. Redfern , Nature, 201, 86, (1964).
24. V. Satava, Thermochim. Acta, 2, 423, (1971).
25. J. Sestak, Phys. Chem. Glass, 15, 137, (1974).
26. C. H. N. Goodman, J. Glass Tech., 28, (1987).

Fig. Captions:

Fig.(1-a): Variation of density with La_2O_3 content (mol.%) for $(TeO_2)_{(100-x)}$-$(La_2O_3)_x$ glasses.

Fig.(1-b): Variation of density with V_2O_5 content (mol.%) for $(TeO_2)_{(100-x)}$-$(V_2O_5)_x$ glasses.

Fig.(2-a): Variation of molar volume with La_2O_3 content (mol.%) for $(TeO_2)_{(100-x)}$-$(La_2O_3)_x$ glasses.

Fig.(2-b): Variation of molar volume with V_2O_5 content (mol.%) for $(TeO_2)_{(100-x)}$-$(V_2O_5)_x$ glasses.

Fig.(3-a): Variation of the molar volume with the Ratio between the number of network formula units (n_B/n_A) for $(TeO_2)_{(100-x)}$-$(La_2O_3)_x$ glasses.

Fig.(3-b): Variation of the molar volume with the Ratio between the number of network formula units (n_B/n_A) for $(TeO_2)_{(100-x)}$-$(V_2O_5)_x$ glasses.

Fig.(4-a): Variation of Nb (the number of bond per unit volume) with La2O3 content (mol.%) for (TeO2)(100-x)-(La2O3)x glasses.

Fig.(4-b): Variation of Nb (the number of bond per unit volume) with V_2O_5 content (mol.%) for $(TeO_2)_{(100-x)}$-$(V_2O_5)_x$ glasses.

Fig.(5-a): Variation of $\overline{F}$ (N/cm) (average force constant) with La_2O_3 content (mol.%) for $(TeO_2)_{(100-x)}$-$(La_2O_3)_x$ glasses.

Fig.(5-b): Variation of $\overline{F}$ (N/cm) (average force constant) with V_2O_5content (mol.%) for $(TeO_2)_{(100-x)}$-$(V_2O_5)_x$ glasses.

Fig.(6-a): Typical DSC traces of the prepared binary lanthanum telluriteglasses for different composition at heating rate 10 K/min.

Fig.(6-b): Typical DSC traces of the prepared binary $(TeO_2)_{90}$-$(La_2O_3)_{10}$ glasses for different heating rate.

Fig.(7-a): Typical DSC traces of the prepared binary vanadium tellurite glasses for different composition at heating rate 10 K/min.

Fig.(7-b): Typical DSC traces of the prepared binary $(TeO_2)_{65}$-$(V_2O_5)_{35}$ glasses for different heating rate.

Fig.(8-a): Variation of T_g vs. Ln(α) for $(TeO_2)_{(100-x)}$-$(La_2O_3)_x$ glasses.

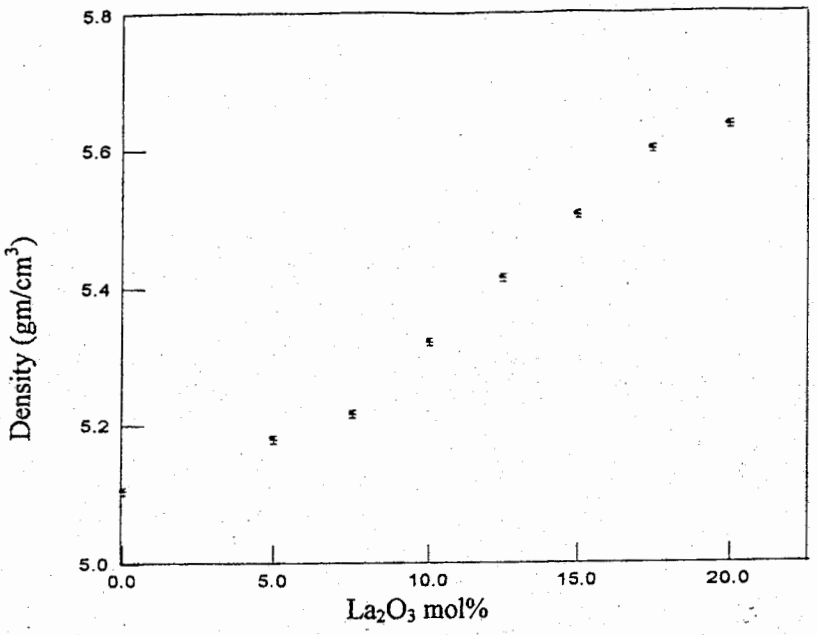

Fig.(1-a): Variation of density with La_2O_3 content (mol.%) for $(TeO_2)_{(100-x)}$-$(La_2O_3)_x$ glasses.

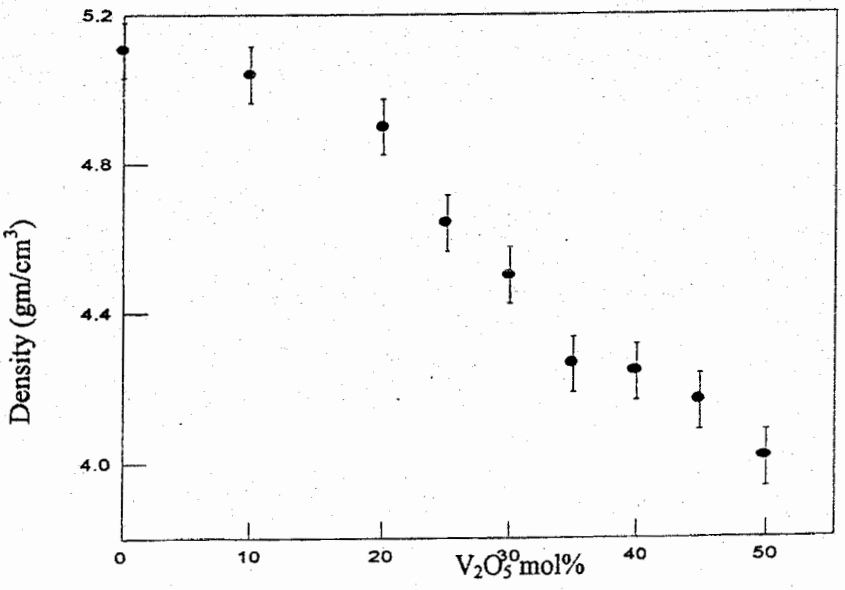

Fig.(1-b): Variation of density with V_2O_5 content (mol.%) for $(TeO_2)_{(100-x)}$-$(V_2O_5)_x$ glasses.

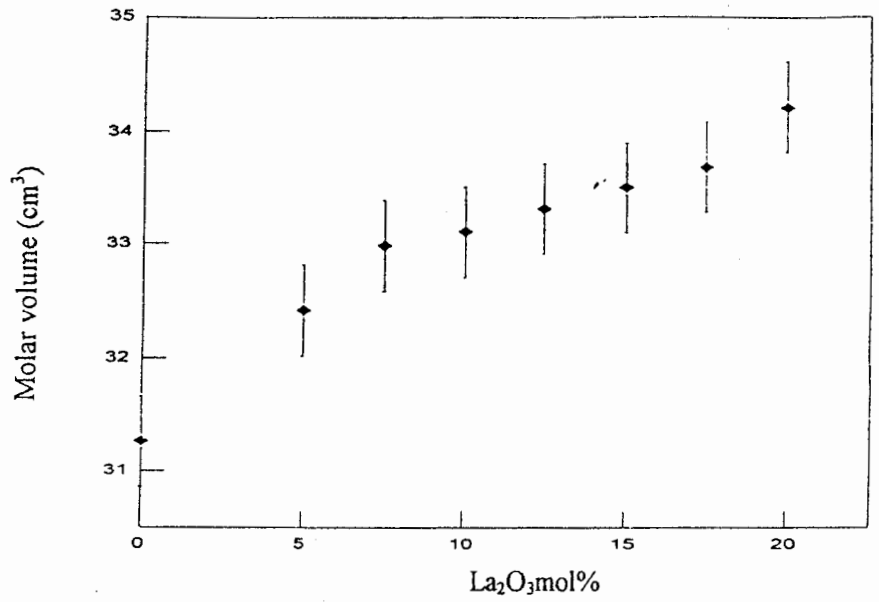

Fig.(2-a): Variation of molar volume with La_2O_3 content (mol.%) for $(TeO_2)_{(100-x)}$-$(La_2O_3)_x$ glasses.

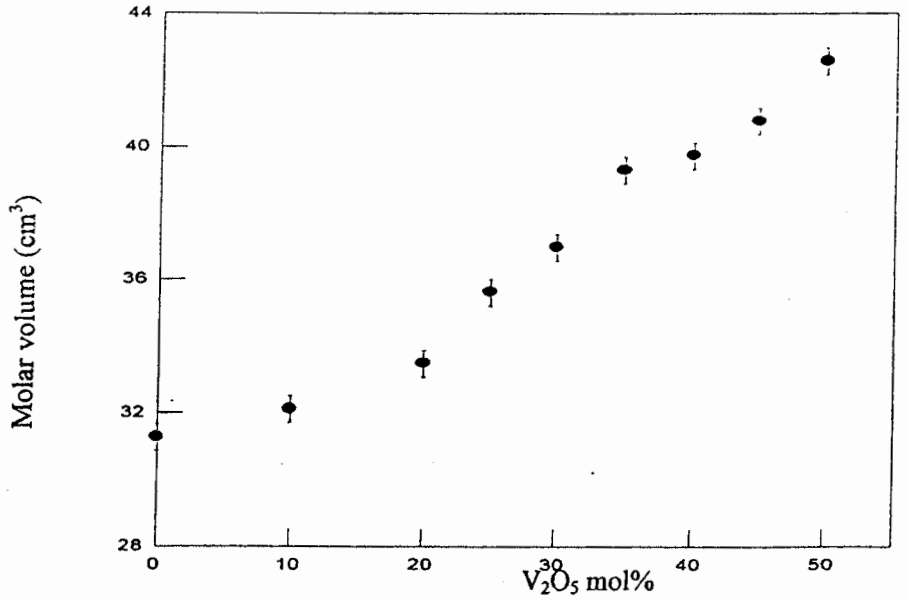

Fig.(2-b): Variation of molar volume with V_2O_5 content (mol.%) for $(TeO_2)_{(100-x)}$-$(V_2O_5)_x$ glasses.

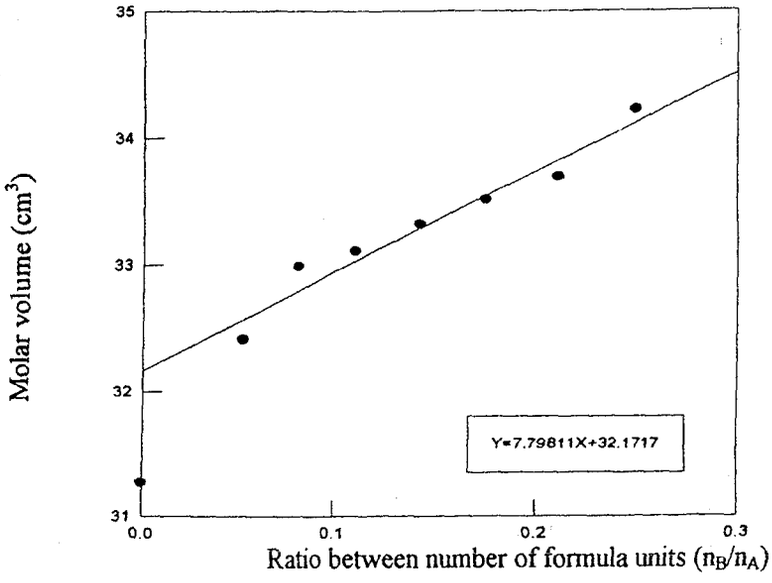

Fig.(3-a): Variation of the molar volume with the Ratio between the number of network formula units (n_B/n_A) for $(TeO_2)_{(100-x)}$-$(La_2O_3)_x$ glasses.

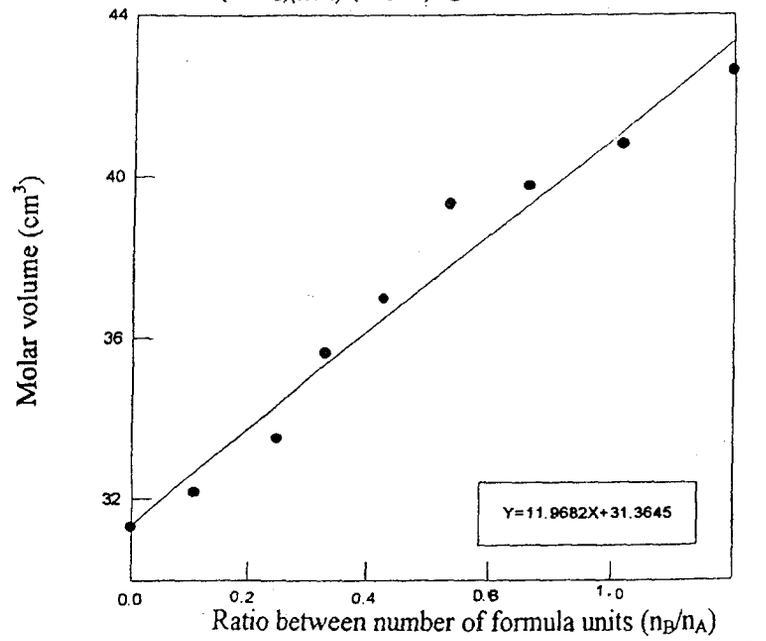

Fig.(3-b): Variation of the molar volume with the Ratio between the number of network formula units (n_B/n_A) for $(TeO_2)_{(100-x)}$-$(V_2O_5)_x$ glasses.

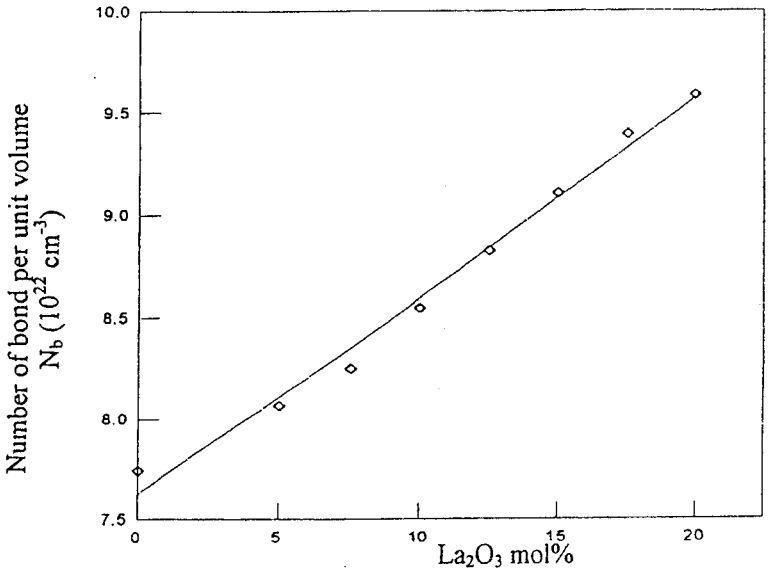

Fig.(4-a): Variation of N_b (the number of bond per unit volume) with La_2O_3 content (mol.%) for $(TeO_2)_{(100-x)}$-$(La_2O_3)_x$ glasses.

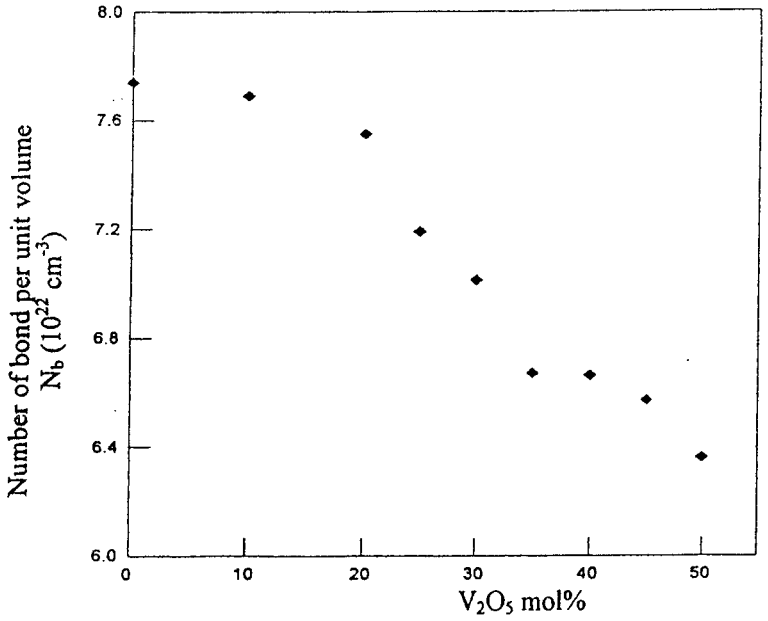

Fig.(4-b): Variation of N_b (the number of bond per unit volume) with V_2O_5 content (mol.%) for $(TeO_2)_{(100-x)}$-$(V_2O_5)_x$ glasses.

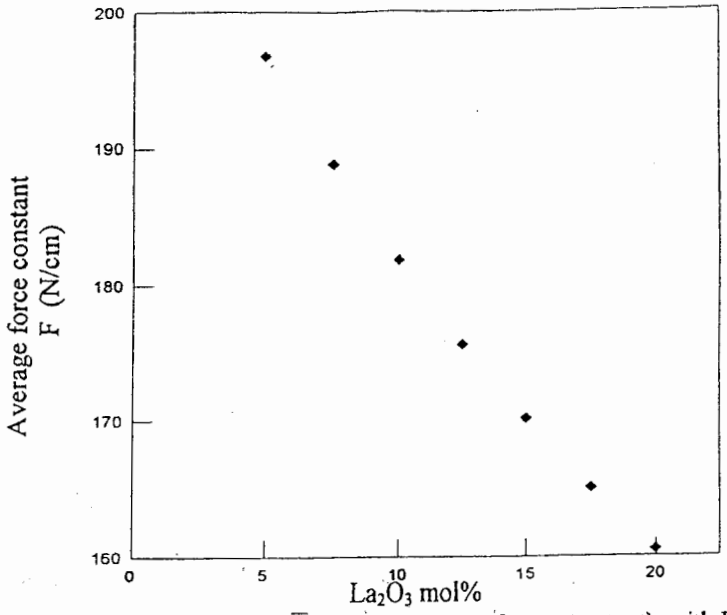

Fig.(5-a): Variation of $\overline{F}$ (N/cm) (average force constant) with La_2O_3 content (mol.%) for $(TeO_2)_{(100-x)}$-$(La_2O_3)_x$ glasses.

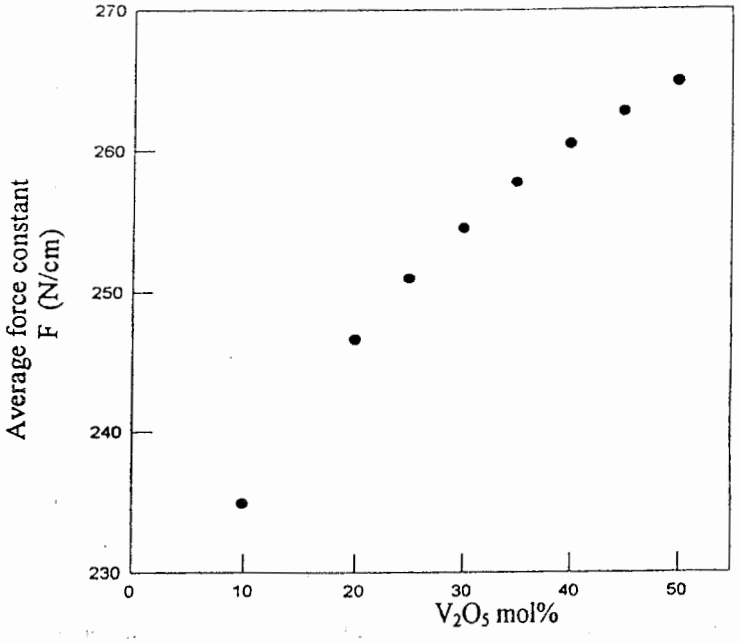

Fig.(5-b): Variation of $\overline{F}$ (N/cm) (average force constant) with V_2O_5 content (mol.%) for $(TeO_2)_{(100-x)}$-$(V_2O_5)_x$ glasses.

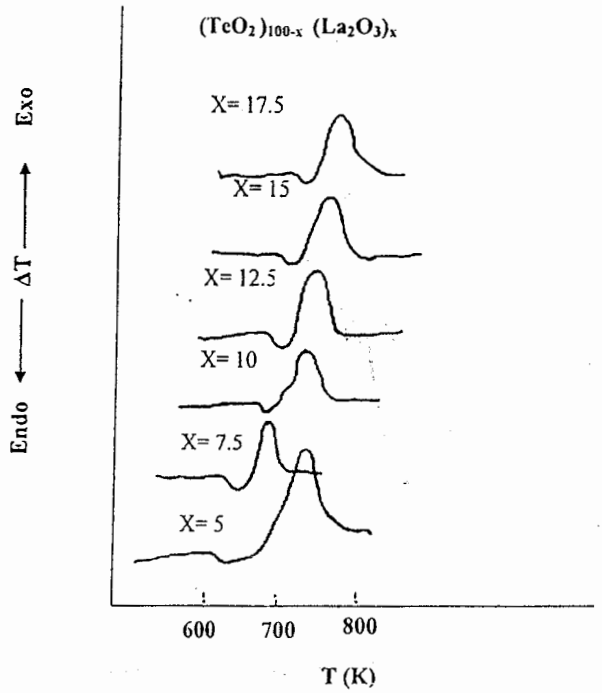

Fig. (6-a): Typical DSC traces of the prepared binary lanthanum tellurite glasses for different composition at heating rate 10 K/min.

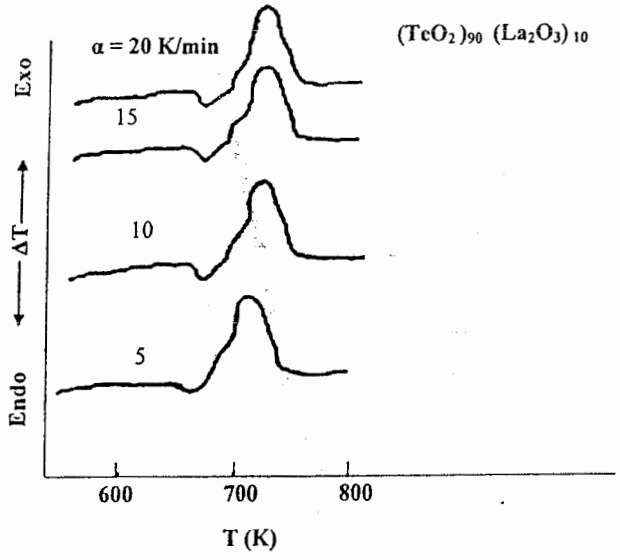

Fig. (6-b): Typical DSC traces of the prepared binary $(TeO_2)_{90}$ $(La_2O_3)_{10}$ glasses for different heating rate.

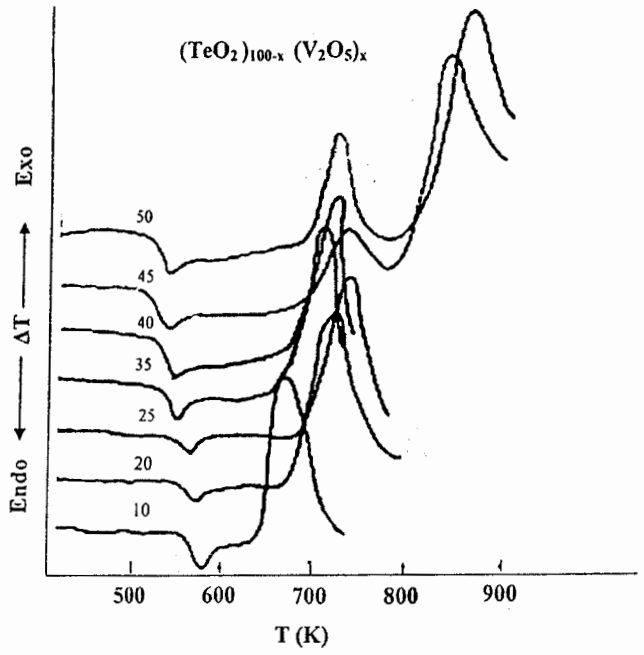

Fig. (7-a): Typical DSC traces of the prepared binary vanadium tellurite glasses for different composition at heating rate 10 K/min.

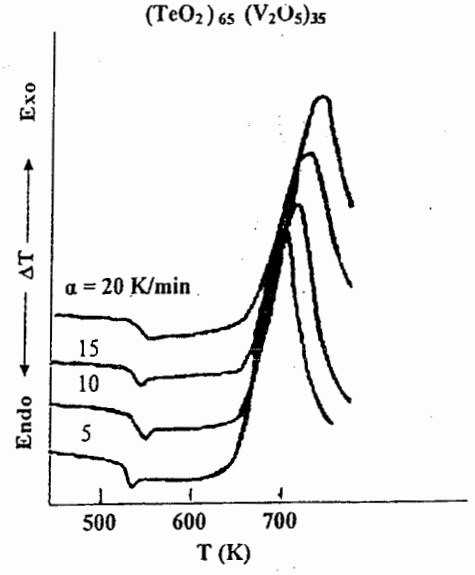

Fig. (7-b): Typical DSC traces of the prepared binary $(TeO_2)_{65}$ $(V_2O_5)_{35}$ glasses for different heating rate.

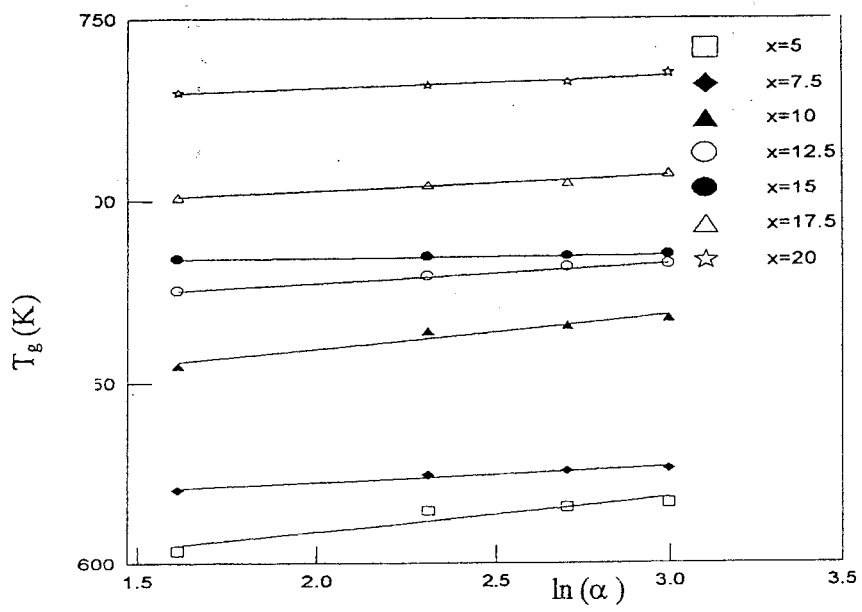

Fig.(8-a): Variation of T_g vs. Ln(α) for $(TeO_2)_{(100-x)}$-$(La_2O_3)_x$ glasses.

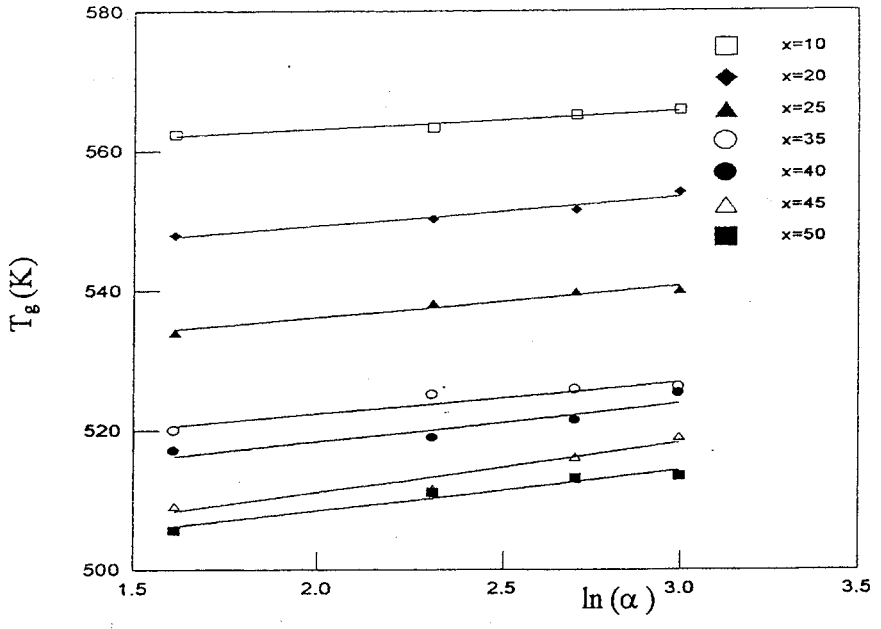

Fig.(8-b): Variation of T_g vs. Ln(α) for $(TeO_2)_{(100-x)}$-$(V_2O_5)_x$ glasses.

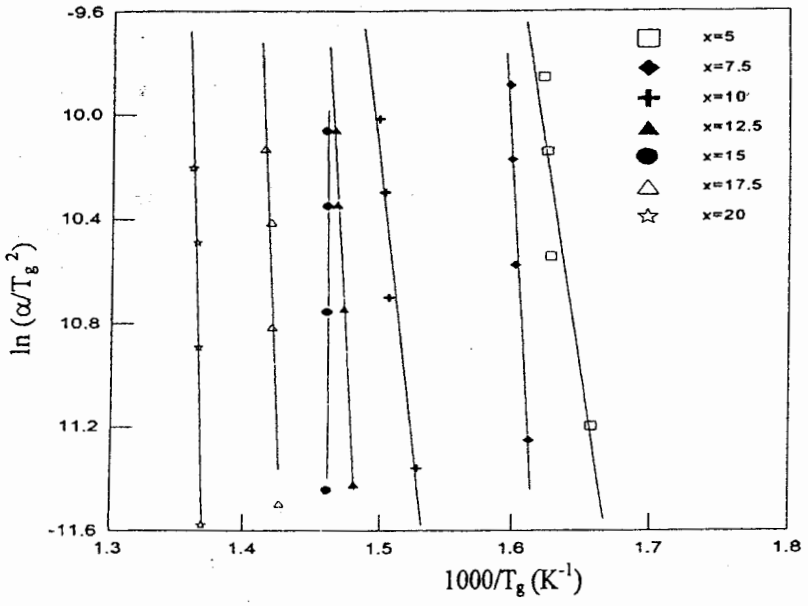

Fig.(9-a): Variation of $\ln(\alpha/T_g^2)$ vs. $(1000/T_g)$ for $(TeO_2)_{(100-x)}$-$(La_2O_3)_x$ glasses.

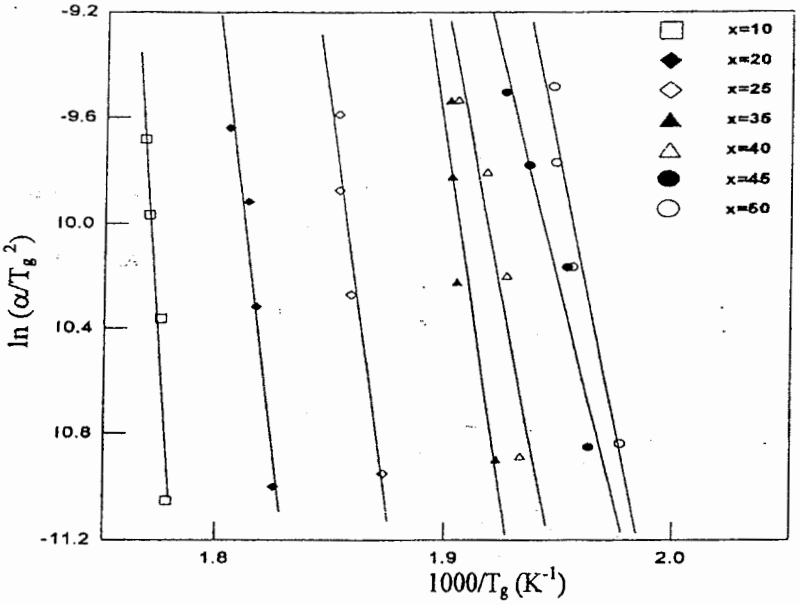

Fig.(9-b): Variation of $\ln(\alpha/T_g^2)$ vs. $(1000/T_g)$ for $(TeO_2)_{(100-x)}$-$(V_2O_5)_x$ gasses.

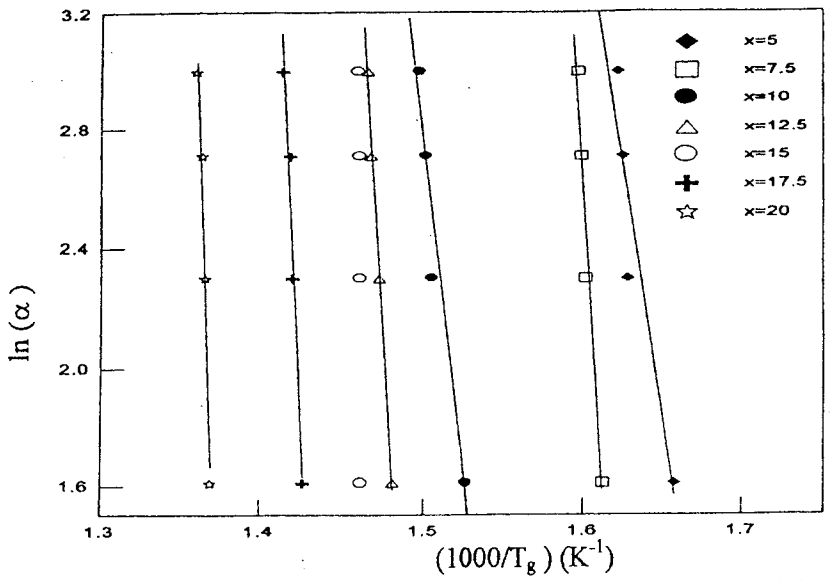

Fig.(10-a): Variation of ln(α) vs. $(1000/T_g)$ for $(TeO_2)_{(100-x)}$-$(La_2O_3)_x$ glasses.

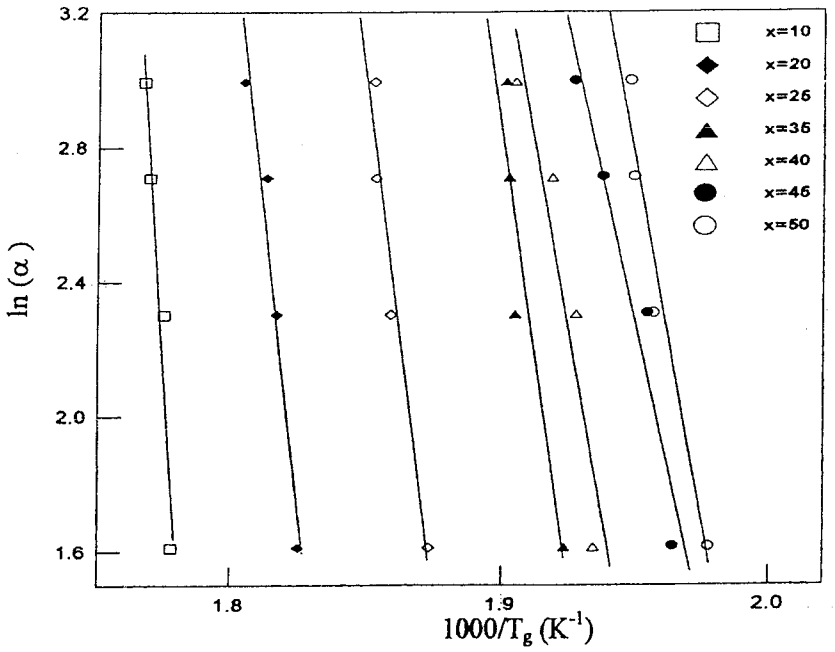

Fig.(10-b): Variation of ln (α) vs. $\{1000/T_g)$ for $(TeO_2)_{(100-x)}$-$(V_2O_5)_x$ glasses.

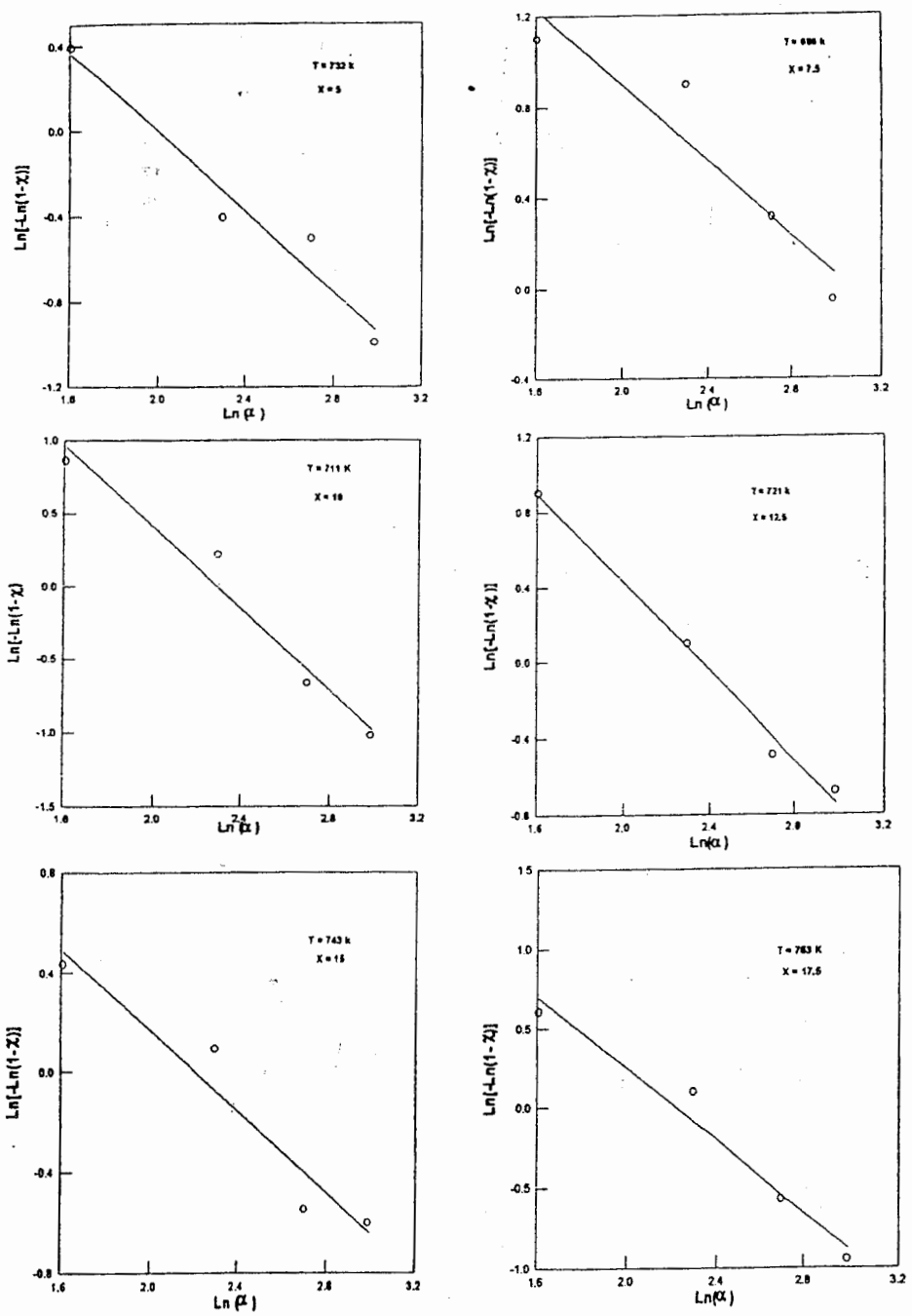

Fig.(11-a): Variation of Ln(-Ln(1-χ)) vs. Ln(α) for $(TeO_2)_{(100-x)}$-$(La_2O_3)_x$ glasses.

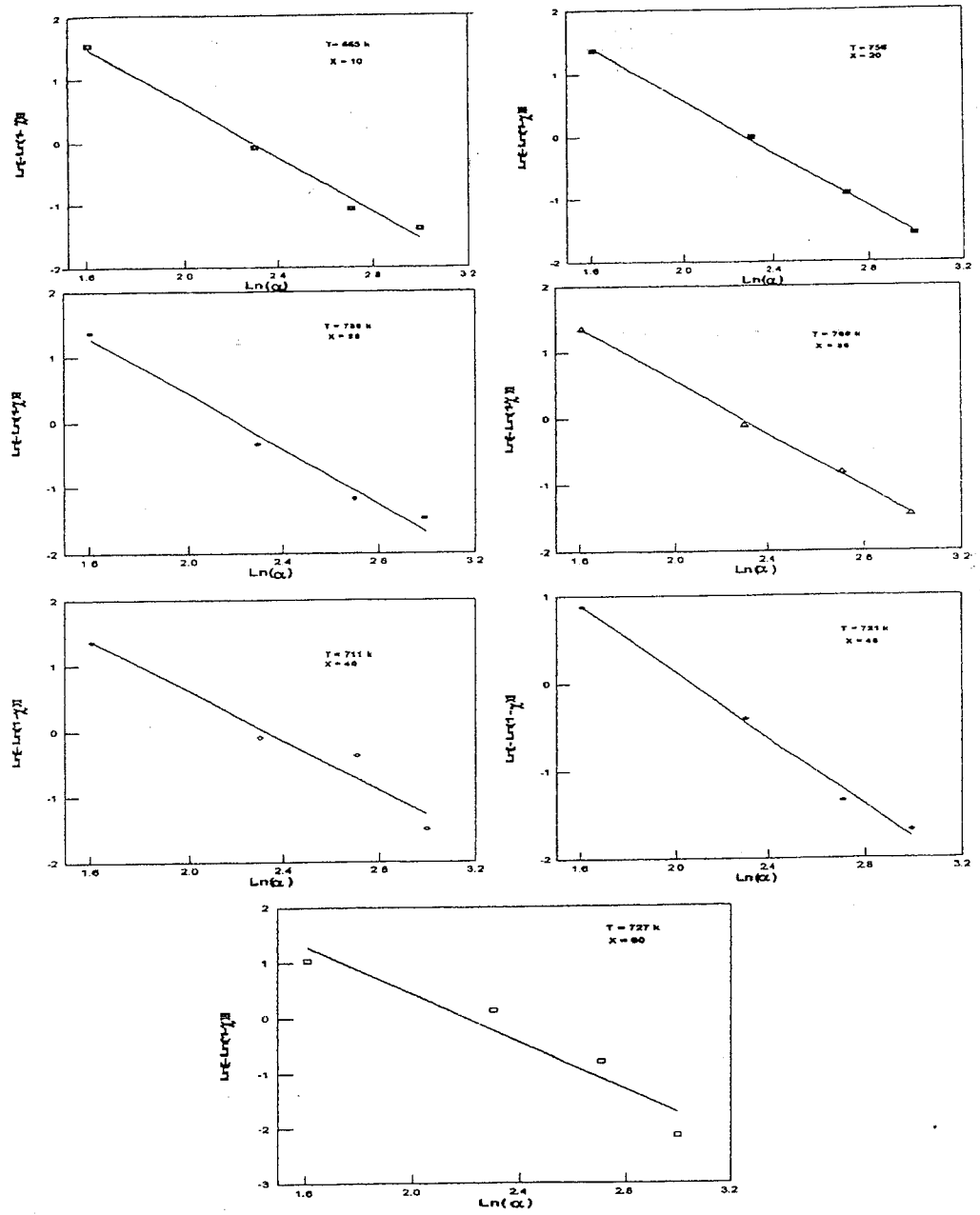

Fig.(11-b): Variation of Ln(-Ln(1-χ)) vs. Ln(α) for $(TeO_2)_{(100-x)}$-$(V_2O_5)_x$ glasses.

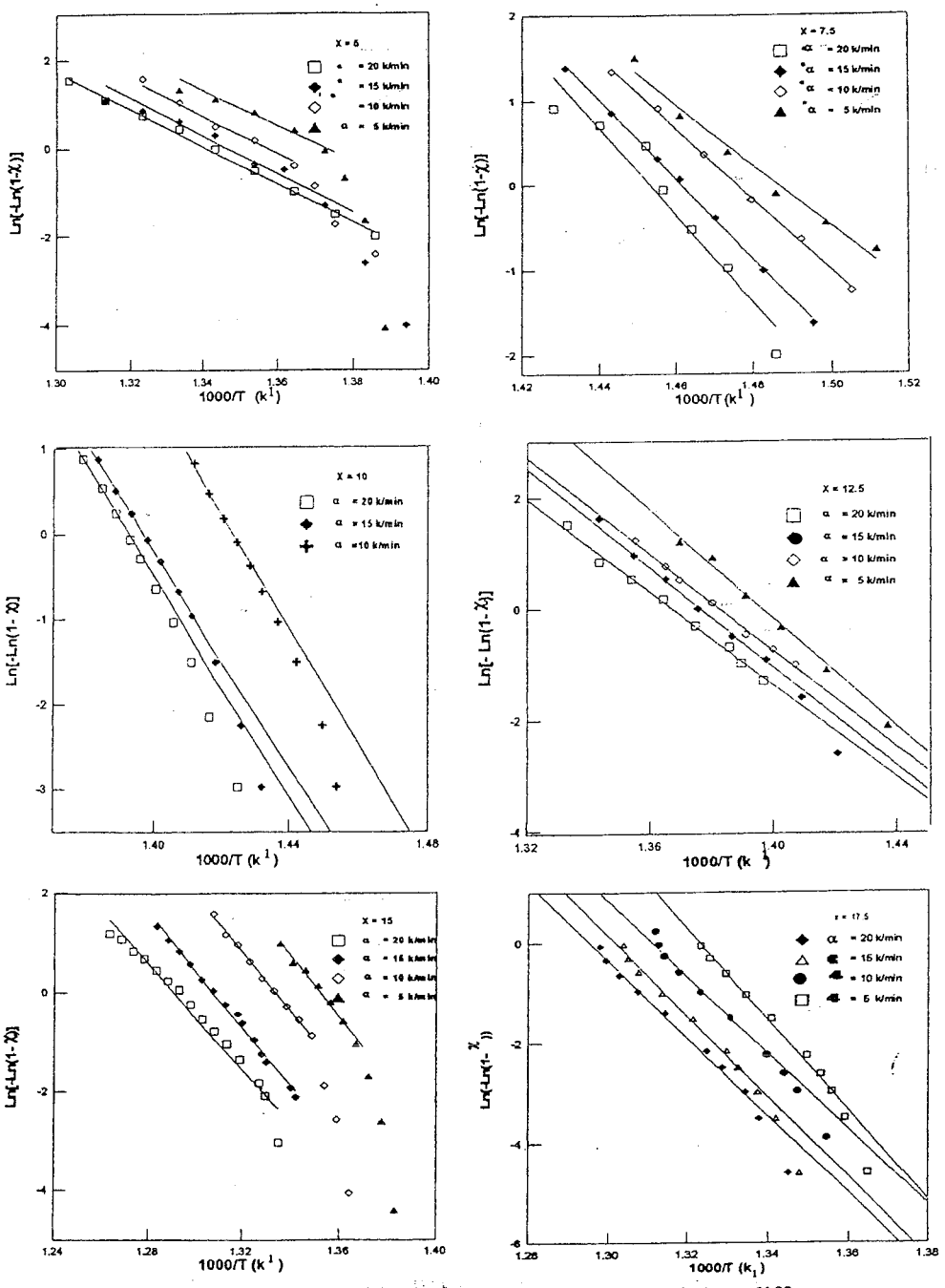

Fig.(12-a): The relation between Ln(-Ln(1-χ)) vs. 1000/T(K) at different heating rates for $(TeO_2)_{(100-x)}$-$(La_2O_3)_x$ glasses

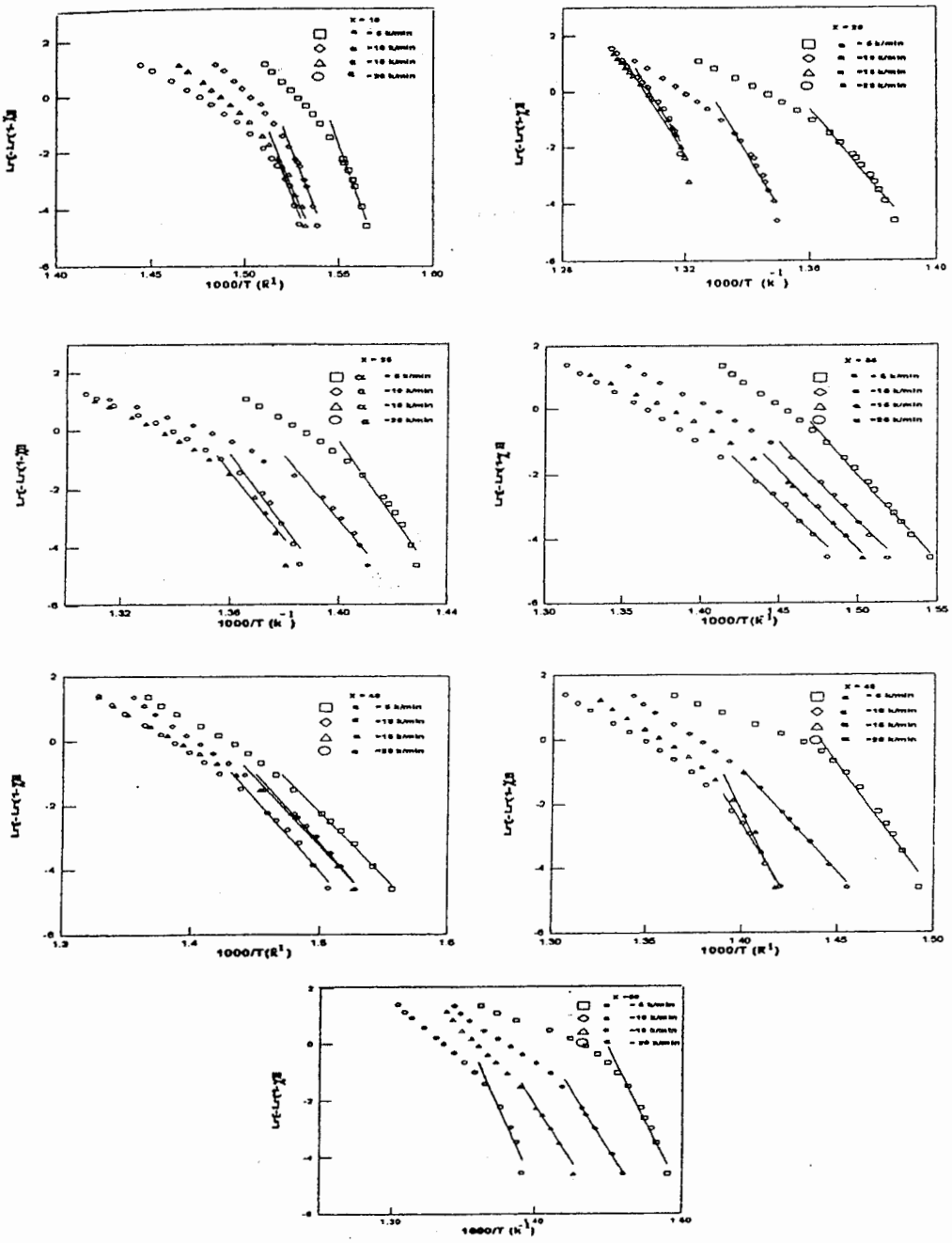

. Fig.(12-b): The relation between Ln(-Ln(1-χ)) vs.(1000/T) at different heating rates for $(TeO_2)_{(100-x)}$-$(V_2O_5)_x$ glasses.

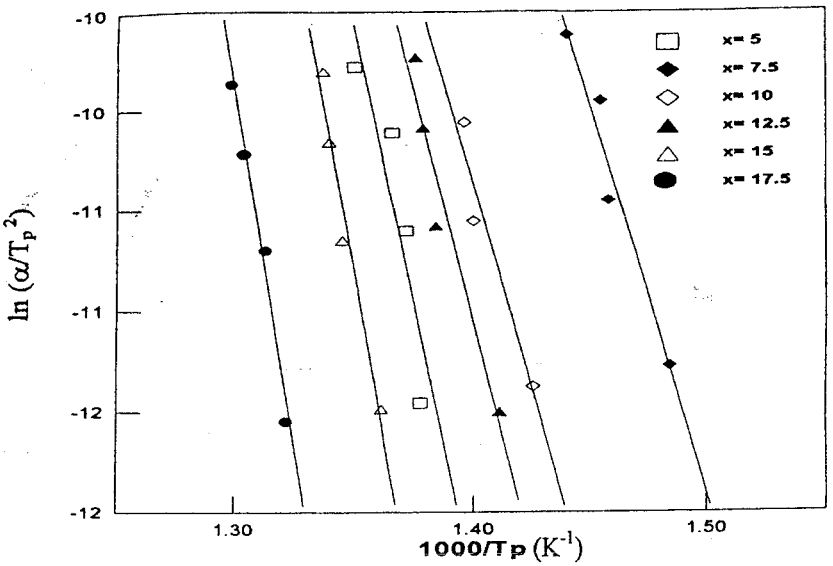

Fig.(13-a): Variation of $Ln(\alpha/T_p^2)$ vs. $(1000/T_p)$ for $(TeO_2)_{(100-x)}$-$(La_2O_3)_x$ glasses.

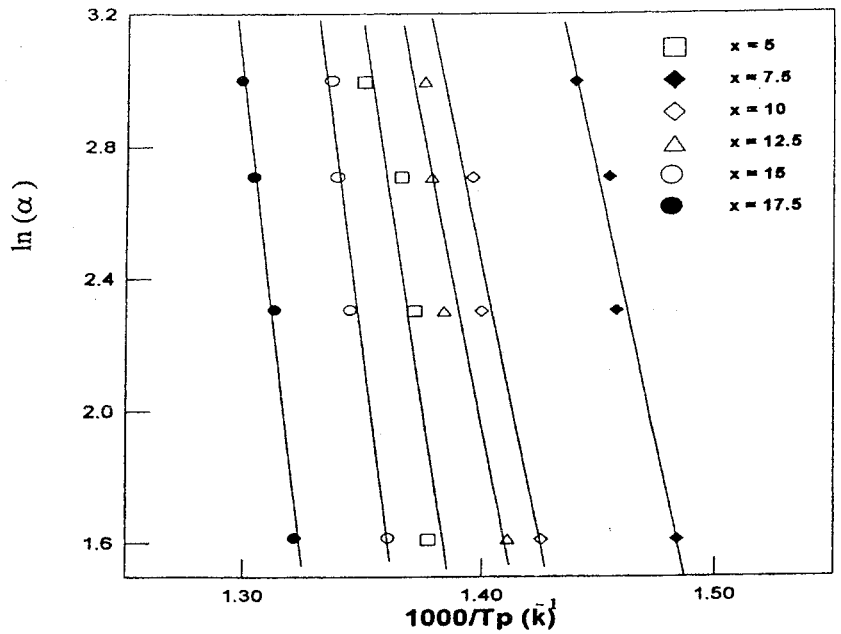

Fig.(14-a): Variation of $Ln(\alpha)$ vs. $(1000/T_p)$ for $(TeO_2)_{(100-x)}$-$(La_2O_3)_x$ glasses.

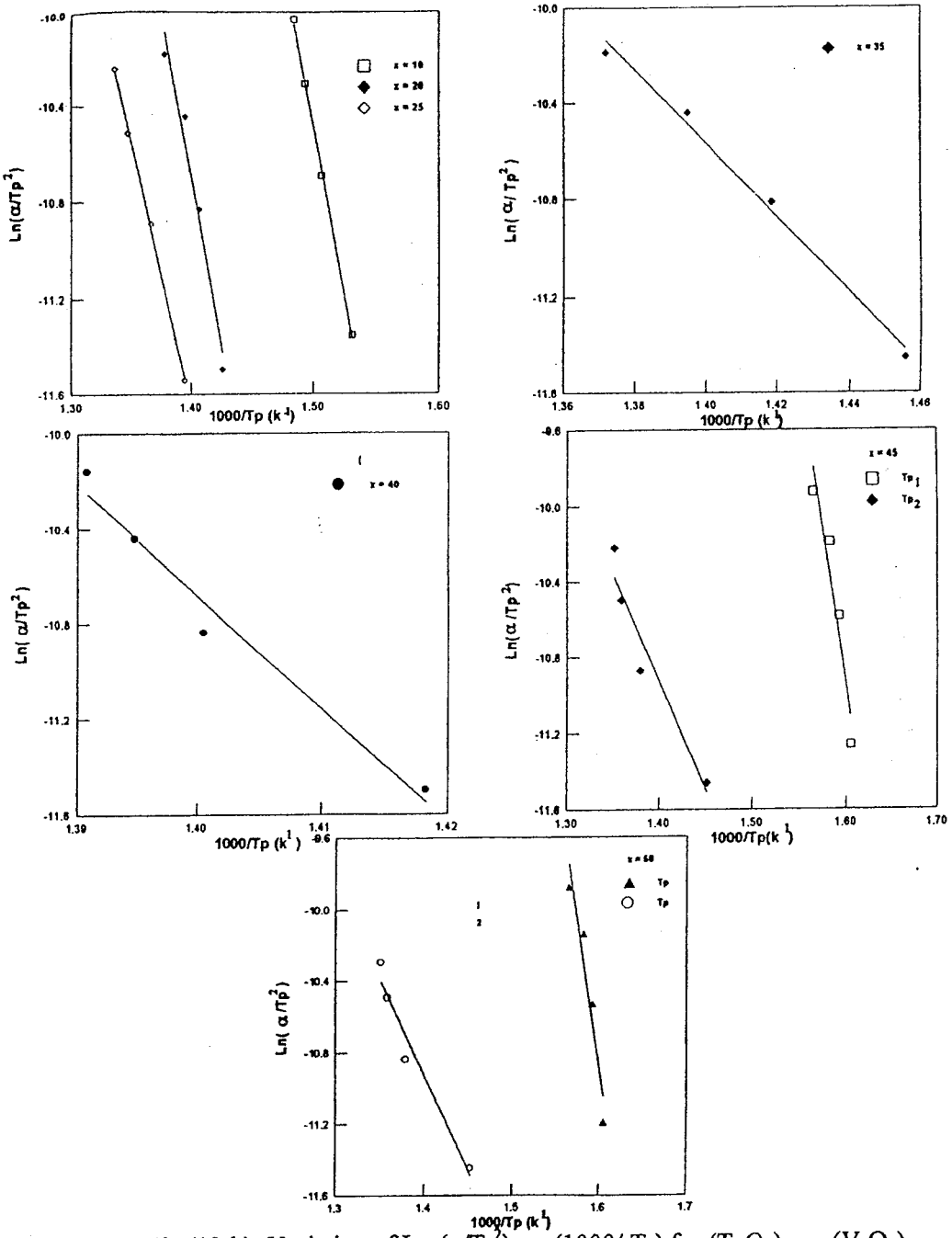

Fig.(13-b): Variation of Ln (α/T_p^2) vs. (1000/ T_p) for $(TeO_2)_{100-x}$-$(V_2O_5)_x$ glasses.

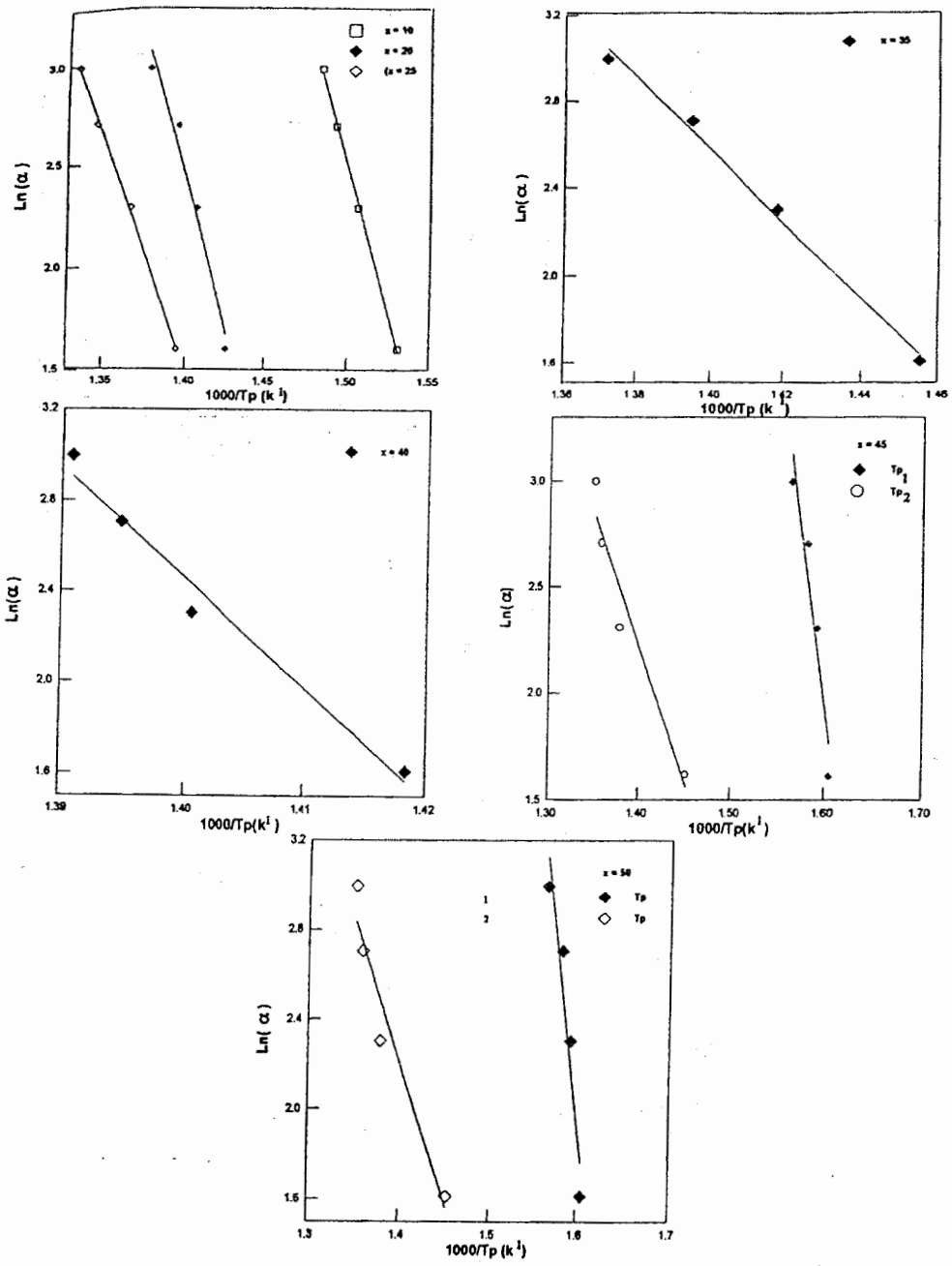

Fig.(14-b): Variation of Ln (α) vs. (1000/ T_p) for $(TeO_2)_{100-x}$-$(V_2O_5)_x$ glasses.

Table (1):

Density, Molar volume, Number of bonds per unit volume and Average force constant of binary tellurite glasses.

Glass Composition	ρ (gm/cm^3) using Eq.(1)	V (cm^3) using Eq.(2)	N_b (10^{22} cm^{-3}) Using Eq.(5)	F (N/cm) using Eq.(6)
TeO2 glass [2,4]	5.105	31.26	7.74	
TeO2 crystal [3,4]	5.99	26.6		
TeO2-La2O3				
95 - 5	5.18	32.42	8.07	196.7
92.5 - 7.5	5.22	32.98	8.25	188.8
90 - 10	5.32	33.11	8.55	181.8
87.5 -12.5	5.42	33.31	8.83	175.6
85 - 15	5.51	33.5	9.11	170.1
82.5 – 17.5	5.60	33.68	9.39	165.0
80 - 20	5.64	34.21	9.58	160.5
TeO2-V2O5				
90 - 10	5.04	32.11	7.69	234.8
80 - 20	4.9	33.48	7.55	246.5
75 - 25	4.64	35.60	7.19	250.9
70 - 30	4.5	36.95	7.01	254.5
65 - 35	4.26	39.30	6.67	257.7
60 - 40	4.24	39.74	6.66	260.4
55 - 45	4.16	40.78	6.57	262.7
50 - 50	4.01	42.58	6.36	264.8

Table (2):

Thermal properties of the binary tellurite glasses.

Glass composition	Tg (K)	Tx (K)	Tc (K)	Tm (K)	Tx-Tg (K)	Tg/Tm	Tc-Tg (K)	Kg= (Tc-Tg)/(Tm-Tc)
TeO2 glass [2]	598	673	713	933	75	0.6	115	0.41
TeO2-La2O3								
95 - 5	615	670	727	917	55	0.67	112	0.59
92.5 - 7.5	624	661	676	923	37	0.68	52	0.21
90 - 10	666	687	726	928	21	0.72	60	0.3
87.5 - 12.5	675	707	735	921	32	0.73	60	0.32
85 - 15	684	708	747	944	24	0.72	63	0.32
82.5 - 17.5	705	730	755	953	25	0.74	50	0.25
TeO2-V2O5								
90 - 10	563	646	664	993	83	0.57	101	0.31
80 - 20	550	664	721	1160	114	0.47	171	0.39
75 - 25	538	676	732	1166	138	0.46	194	0.45
65 - 35	525	652	705	1170	127	0.45	180	0.39
60 - 40	519	677	714	1173	158	0.44	195	0.42
55 - 45	512	685	724	1178	173	0.43	212	0.47
50 - 50	511	686	714	1180	175	0.43	203	0.44

Table (3):

The glass transition temperature and the glass transition activation energies of binary tellurite glasses.

Glass Composition	T_g (K)	E_t (kJ/mol) Using eq.(10)	Et (kJ/mol) Using eq.(11)
TeO2 - La2O3			
95 - 5	615	276.38	286.5
92.5 – 7.5	624	285.71	296
90 – 10	666	291.67	302.31
87.5 – 12.5	675	355.06	366.3
85 – 15	684	390.34	401.8
82.5 – 17.5	705	392.32	403.9
80 – 20	733	411.67	423.7
TeO2 - V2O5			
90 - 10	563	585.58	594.96
80 - 20	550	571.16	580.32
75 - 25	538	500.31	509.24
65 - 35	525	436.12	446.82
60 - 40	519	351.99	360.65
55 - 45	512	344.01	352.48
50 - 50	511	281.25	289.79

Table (4):

Obtained data m, n and E_c (kJ/mol) in the binary tellurite glasses .

Glass Composition	n_1	n_2	m	Ec (kJ/mol)	Ec (kJ/mol)	Ec (kJ/mol)
(TeO_2-La_2O_3)						
95 - 5	0.93		1	348.36	342.14	353.53
92.5- 7.5	0.83		1	366.6	347.77	363.35
90 - 10	1.40		1	373.5	376.74	372.18
87.5-12.5	1.18		1	371.6	370.79	359.88
85 - 15	0.81		1	483.66	461.43	474.39
82.5-17.5	1.14		1	557.04	531.75	546.17
(TeO2 - V2O5)						
90 - 10	2.17		1	486.37	458.93	486.37
80 - 20	2.11		1	471.40	453.94	468.7
75 - 25	2.12		1	371.64	357.50	376.73
65 - 35	2.01		1	333.39	320.92	346.27
60 - 4	1.91		1	300.14	274.36	266.04
55 - 45	1.90	2.33	1	207.85	191.22	204.44
50 - 50	2.17	3.31	1	177.09	174.59	198.2